GW quasiparticle energies of atoms in strong magnetic fields

Christof Holzer,[1] Andrew M. Teale,[2,3,4] Florian Hampe,[5] Stella Stopkowicz,[3,5] Trygve Helgaker,[3,4] Wim Klopper*[1,3]

[1] *Karlsruhe Institute of Technology (KIT), Institute of Physical Chemistry, KIT Campus South, P. O. Box 6980, D-76049 Karlsruhe, Germany*

[2] *University of Nottingham, School of Chemistry, University Park, Nottingham NG7 2RD, United Kingdom*

[3] *Centre for Advanced Study (CAS) at The Norwegian Academy of Science and Letters, Drammensveien 78, N-0271 Oslo, Norway*

[4] *Hylleraas Centre for Quantum Molecular Sciences, Department of Chemistry, University of Oslo, P. O. Box 1033, N-0315 Oslo, Norway*

[5] *Johannes Gutenberg-Universität Mainz, Institute of Physical Chemistry, D-55099 Mainz, Germany*

* *Corresponding author, e-mail: klopper@kit.edu*

Quasiparticle energies of the atoms H–Ne have been computed in the *GW* approximation in the presence of strong magnetic fields with field strengths varying from 0 to 0.25 atomic units ($0.25\,B_0 = 0.25\,\hbar e^{-1}a_0^{-2} \approx 58763$ T). The *GW* quasiparticle energies are compared with equation-of-motion ionization-potential (EOM-IP) coupled-cluster singles-and-doubles (CCSD) calculations of the first ionization energies. The best results are obtained with the ev*GW*@PBE0 method, which agrees with the EOM-IP-CCSD model to within about 0.20 eV. Ionization potentials have been calculated for all atoms in the series, representing the first systematic study of ionization potentials for the first-row atoms at field strengths characteristic of magnetic white dwarf stars. Under these conditions, the ionization potentials increase in a near-linear fashion with the field strength, reflecting the linear field dependence of the Landau energy of the ionized electron. The calculated ionization potentials agree well with the best available literature data for He, Li, and Be.

Keywords: Magnetic field, *GW* approximation, quasiparticle energy, ionization energy

I. INTRODUCTION

The study of atoms in strong magnetic fields is motivated by the existence of strong magnetic fields on white dwarf stars (up to about 10^5 T), neutron stars (up to about 10^8 T), and magnetars (up to about 10^{11} T). An important aspect of such studies is to understand the relative abundance of neutral and ionized atomic species under prevalent conditions. It is then necessary to know the ionization energies of atoms in magnetic fields. We here present calculations of ionization energies from *GW* quasiparticle energies, which are compared with highly accurate equation-of-motion ionization-potential (EOM-IP) coupled-cluster singles-and-doubles (CCSD) results and literature data. We restrict ourselves to field strengths up to 0.25 B_0 (where $B_0 = \hbar e^{-1}a_0^{-2} \approx 2.3505 \times 10^5$ T is the atomic unit of magnetic field strength), characteristic of white dwarfs. For a recent review of the observational and theoretical characteristics of magnetic white dwarfs, see Ref. 1.

Atoms in strong magnetic fields have been studied using a number of techniques. Early work has been reviewed by Schmelcher[2] and Lai,[3] while more recent work is covered by Thirumalai and Heyl.[4] The first systematic investigation of atoms in the He–Ne series in strong magnetic fields was carried out by Ivanov and Schmelcher using their two-dimensional mesh Hartree–Fock method.[5–8] The lighter atoms in this series have also been studied at higher levels of theory, including full configuration-interaction (FCI) studies of Schmelcher and coworkers of the helium atom,[9–11] the lithium atom,[12] and the beryllium atom.[13] Recently, Wunner and coworkers have studied the neutral He–Fe series[14] and the ions in the He–Ne series[15] in a magnetic field using a diffusion Monte Carlo (DMC) technique. Stopkowicz and coworkers investigated atoms in strong magnetic fields using the coupled-cluster singles-and-doubles (CCSD) model and the CCSD-perturbative-triples (CCSD(T)) model in 2015,[16] and using the coupled-cluster equation-of-motion (EOM) method at the CCSD level in 2017.[17] The lighter atoms helium and lithium have been studied using Hylleraas-type explicitly correlated methods,[18–20] while the variational Monte Carlo method has been applied to helium[21] and lithium.[22] We also mention here the pseudospectral Hartee–Fock method of Thirumalai and Heyl for neutron-strength magnetic fields.[23] Many of the studies above concern not only the total energies of ground or excited states but also ionization energies.[5–15,21,22]

In the present paper, we calculate the ionization potentials (IPs) of the electronic ground states of the atoms in the series He–Ne using a recently developed *GW* mod-

ule within the TURBOMOLE[24] and QUEST[25,26] packages, comparing with EOM-IP-CCSD results obtained using the coupled-cluster code of Hampe and Stopkowicz[17] interfaced with the LONDON program.[27,28] When available, we compare with literature data.

The remainder of this paper is structured as follows. In Section II, we review the *GW* and EOM-IP-CCSD methods with focus on aspects related to the use of complex variables. Computational details are given in Section III, while results are presented and discussed in Section IV. Some concluding remarks are made in Section V.

II. THEORY

A. Hamiltonian

We will be concerned with the atomic electronic Hamiltonian for infinite nuclear mass in a uniform and constant magnetic field $\mathbf{B}$. For the symmetric gauge of the vector potential, the following one-electron operator is added to the Kohn–Sham or Fock operator (in atomic units):

$$\hat{h}(\mathbf{B}) = \frac{1}{2}\mathbf{B}\cdot\left(\hat{\boldsymbol{\ell}} + 2\hat{\mathbf{s}}\right) + \frac{1}{8}\left(\mathbf{B}\times\mathbf{r}\right)^2 , \tag{1}$$

where $\frac{1}{2}\mathbf{B}\cdot\hat{\boldsymbol{\ell}}$ and $\mathbf{B}\cdot\hat{\mathbf{s}}$ are the orbital and spin Zeeman terms, respectively, and where $\frac{1}{8}\left(\mathbf{B}\times\mathbf{r}\right)^2$ is the diamagnetic term.

We will choose the magnetic field along the z-axis and perform unrestricted Hartree–Fock and Kohn–Sham calculations, in which the orbitals are eigenfunctions of the operators $\hat{\ell}_z$ and $\hat{s}_z$ with quantum numbers m_ℓ and m_s, respectively. Accordingly, the corresponding (Hartree–Fock or Kohn–Sham) determinant is an eigenfunction of the z projections $\hat{L}_z$ and $\hat{S}_z$ of total angular momentum and total spin with quantum numbers M_L and M_S, respectively.

For very large field strengths (much larger than 1 B_0), finite nuclear mass and center-of-mass corrections to IPs become important,[29,30] but for the field strengths considered by us, corrections beyond the infinite nuclear mass approximation can be neglected.

B. *GW* approach

The *GW* approach provides direct access to the atom's ionization energies, which are obtained as the negatives of its quasiparticle energies. We have therefore generalized the *GW* approach for use on atoms in a finite magnetic field. The main purpose of the present section is to provide correct expressions for *GW* computations using complex-valued quantities (*e.g.*, spinors). Note that in the present work's formulation, the numerator of the first term on the right hand side of Eq. (11) reads $V_m^*(\mathbf{x})V_m(\mathbf{x}')\phi_k(\mathbf{x})\phi_k^*(\mathbf{x}')$, whereas the corresponding numerator of Ref. 31 reads $V_m(\mathbf{r})V_m^*(\mathbf{r}')\phi_l(\mathbf{x})\phi_l^*(\mathbf{x}')$. It is important to note that equation 10 of Ref. 31 cannot be used when complex-valued quantities occur in the theory. Instead, Eq. (11) of the present work should be used.

We nevertheless closely follow Ref. 31 and define the charge-fluctuation potential

$$V_m(\mathbf{x}) = \int_{-\infty}^{\infty} v(\mathbf{r}-\mathbf{r}')\rho_m(\mathbf{x}')\mathrm{d}\mathbf{x}' , \tag{2}$$

where m denotes an excited state, where $v(\mathbf{r}) = 1/|\mathbf{r}|$ is the Coulomb potential, and where the space-spin-coordinate $\mathbf{x} \equiv (\mathbf{r},\sigma)$ includes both space and spin coordinates. The charge fluctuation is given as

$$\rho_m(\mathbf{x}) = \sum_{ia}\left[\phi_a^*(\mathbf{x})\phi_i(\mathbf{x})X_{ia}^m + \phi_i^*(\mathbf{x})\phi_a(\mathbf{x})Y_{ia}^m\right] . \tag{3}$$

Here and in the following, we use the indices $i, j, k, \ldots$ for occupied spinors, $a, b, c, \ldots$ for unoccupied (virtual) spinors, and $p, q, r, \ldots$ for arbitrary spinors.

In Eq. (3), X_{ia}^m and Y_{ia}^m refer to the elements "ia" of the m^{th} columns of the matrices $\mathbf{X}$ and $\mathbf{Y}$, which are obtained by solving the direct random-phase approximation (dRPA) equation

$$\begin{pmatrix} \mathbf{A} & \mathbf{B} \\ -\mathbf{B}^* & -\mathbf{A}^* \end{pmatrix}\begin{pmatrix} \mathbf{X} & \mathbf{Y}^* \\ \mathbf{Y} & \mathbf{X}^* \end{pmatrix} = \begin{pmatrix} \mathbf{X} & \mathbf{Y}^* \\ \mathbf{Y} & \mathbf{X}^* \end{pmatrix}\begin{pmatrix} \boldsymbol{\omega} & \mathbf{0} \\ \mathbf{0} & -\boldsymbol{\omega} \end{pmatrix} , \tag{4}$$

with

$$\mathbf{X}^\dagger\mathbf{X} - \mathbf{Y}^\dagger\mathbf{Y} = \mathbf{1} . \tag{5}$$

On its diagonal, the matrix $\boldsymbol{\omega}$ contains the real-valued dRPA energies ω_m of the excited states m, and the elements of the matrices $\mathbf{A}$ and $\mathbf{B}$ are given as

$$A_{ia,jb} = (\varepsilon_a - \varepsilon_i)\delta_{ij}\delta_{ab} + (ia|bj) , \tag{6a}$$
$$B_{ia,jb} = (ia|jb) , \tag{6b}$$

where ε_p is the energy level of the spinor ϕ_p, and where the two-electron integrals are written in Mulliken notation,

$$(pq|rs) = \iint \phi_p^*(\mathbf{x})\phi_q(\mathbf{x})v(\mathbf{r}-\mathbf{r}')\phi_r^*(\mathbf{x}')\phi_s(\mathbf{x}')\mathrm{d}\mathbf{x}\mathrm{d}\mathbf{x}' . \tag{7}$$

The correlation contribution to the optical potential in the *GW* approximation is

$$\begin{aligned}\Sigma_c(\mathbf{x},\mathbf{x}';\omega) = -\frac{1}{2\pi\mathrm{i}}\int_{-\infty}^{\infty} e^{\mathrm{i}\omega' 0^+} W_c(\mathbf{x},\mathbf{x}';\omega') \\ \times G(\mathbf{x},\mathbf{x}';\omega+\omega')\mathrm{d}\omega' ,\end{aligned} \tag{8}$$

where G is the one-electron Green's function

$$G(\mathbf{x},\mathbf{x}';\omega) = \sum_p \frac{\phi_p(\mathbf{x})\phi_p^*(\mathbf{x}')}{\omega - \varepsilon_p + \mathrm{i}\delta\mathrm{sgn}(\varepsilon_p - \mu)} . \tag{9}$$

Here, δ is a small positive number. The Fermi-level chemical potential μ is chosen to lie between the energy levels of the lowest unoccupied and highest occupied spinors, and W_c is the correlation contribution to the linearly screened potential,

$$W_c(\mathbf{x},\mathbf{x}';\omega) = \sum_{m\neq 0}\left[\frac{V_m^*(\mathbf{x})V_m(\mathbf{x}')}{\omega-\omega_m+\mathrm{i}\delta} - \frac{V_m(\mathbf{x})V_m^*(\mathbf{x}')}{\omega+\omega_m-\mathrm{i}\delta}\right]. \tag{10}$$

The ω' integration in Eq. (8) is most easily carried out by applying Cauchy's residue theorem, yielding

$$\begin{aligned}\Sigma_c(\mathbf{x},\mathbf{x}';\omega) = &\sum_k\sum_{m\neq 0}\frac{V_m^*(\mathbf{x})V_m(\mathbf{x}')\phi_k(\mathbf{x})\phi_k^*(\mathbf{x}')}{\omega+\omega_m-\varepsilon_k-\mathrm{i}\eta}\\ &+\sum_c\sum_{m\neq 0}\frac{V_m(\mathbf{x})V_m^*(\mathbf{x}')\phi_c(\mathbf{x})\phi_c^*(\mathbf{x}')}{\omega-\omega_m-\varepsilon_c+\mathrm{i}\eta},\end{aligned} \tag{11}$$

where $\eta = 2\delta$. We thus obtain the following working equation for the real-valued correlation contribution to the quasiparticle energy:

$$\begin{aligned}\langle p|\Sigma_c(\varepsilon_p)|p\rangle = &\sum_k\sum_{m\neq 0}|(pk|\rho_m)|^2 D^+_{p,k,m}\\ &+\sum_c\sum_{m\neq 0}|(cp|\rho_m)|^2 D^-_{p,c,m},\end{aligned} \tag{12}$$

with

$$D^{\pm}_{p,q,m} = \frac{\varepsilon_p-\varepsilon_q\pm\omega_m}{(\varepsilon_p-\varepsilon_q\pm\omega_m)^2+\eta^2}. \tag{13}$$

The two-electron integrals $(pq|\rho_m)$ are computed as

$$(pq|\rho_m) = \sum_{ia}\left[(pq|ai)X^m_{ia} + (pq|ia)Y^m_{ia}\right]. \tag{14}$$

Eq. (12) is the central result of the present work. Note that the spinor product $\phi_p^*(\mathbf{x})\phi_k(\mathbf{x})$ occurs in the first term on the right-hand side of the equation while $\phi_c^*(\mathbf{x})\phi_p(\mathbf{x})$ occurs in the second term. The complex conjugate of the spinor ϕ_p occurs in the first product but not in the second. Obviously, correct complex conjugation is essential when an external magnetic field is applied.

The exchange self-energy is

$$\langle p|\Sigma_x|p\rangle = -\sum_k(pk|kp), \tag{15}$$

and in the eigenvalue-only self-consistent GW approach (evGW),[32] the quasiparticle energies are computed by means of the iterative scheme

$$\varepsilon_p^{(n+1)} = \varepsilon_p^{(0)} + \langle p|\Sigma_c(\varepsilon_p^{(n)}) + \Sigma_x - V_{\mathrm{xc}}|p\rangle, \tag{16}$$

which starts with Kohn–Sham energies, $\varepsilon_p^{(0)} = \varepsilon_p^{\mathrm{KS}}$, and where V_{xc} is the exchange–correlation potential of the underlying Kohn–Sham method. Note that *all* energies ε_p are updated in each iteration.

The (linearized) G_0W_0 quasiparticle energies are computed as[33,34]

$$\varepsilon_p^{G_0W_0} = \varepsilon_p^{(0)} + Z_p\langle p|\Sigma_c(\varepsilon_p^{(0)}) + \Sigma_x - V_{\mathrm{xc}}|p\rangle, \tag{17}$$

with

$$Z_p = \left\{1 - \langle p|(\partial\Sigma_c(\varepsilon)/\partial\varepsilon)_{\varepsilon=\varepsilon_p^{(0)}}|p\rangle\right\}^{-1}. \tag{18}$$

C. EOM-IP-CCSD approach

The starting point for equation-of-motion coupled-cluster theory for ionization potentials (EOM-IP-CC) is the coupled-cluster wave function

$$|\Psi_{\mathrm{CC}}\rangle = \mathrm{e}^{\hat{T}}|\Phi_0\rangle, \tag{19}$$

where Φ_0 is a reference Slater determinant (usually the Hartree–Fock determinant), and where

$$\hat{T} = \hat{T}_1 + \hat{T}_2 + \ldots, \tag{20a}$$

$$\hat{T}_n = \left(\frac{1}{n!}\right)^2 \sum_{ij\ldots}\sum_{ab\ldots} t_{ij\ldots}^{ab\ldots}\hat{a}_a^\dagger\hat{a}_b^\dagger\ldots\hat{a}_j\hat{a}_i \tag{20b}$$

is the cluster operator.[35,36] In the presence of a magnetic field, Ψ_{CC} will be complex.[16,17] As described in Ref. 35, the coupled-cluster equations for a given N-electron wave function are solved, yielding the amplitudes $t_{ij\ldots}^{ab\ldots}$.

Using $\hat{T}$, the similarity transformed Hamiltonian $\bar{H} = \mathrm{e}^{-\hat{T}}\hat{H}\mathrm{e}^{\hat{T}}$ is formed, which preserves the eigenvalue spectrum of $\hat{H}$. In the presence of a magnetic field, $\hat{H}$ contains the one-electron operators given in Eq. (1). Diagonalization in a basis constructed from $(N-1)$-electron determinants $\{\Phi_\mu\}$ using a modified Davidson method for non-Hermitian matrices yields both the parameters to describe the final wave functions Ψ_n and the corresponding energies E_n,

$$\bar{\mathbf{H}}\mathbf{r}_n = E_n\mathbf{r}_n. \tag{21}$$

The eigenvector $\mathbf{r}_n$ contains the amplitudes $r_{\mu,n}$ that parametrize the final wave function

$$|\Psi_n\rangle = \hat{\mathcal{R}}_n|\Psi_{\mathrm{CC}}\rangle, \tag{22}$$

where $\hat{\mathcal{R}}_n$ is an operator containing strings of quasiparticle creation operators $\hat{\Omega}_\mu$ that produce the determinants spanning the diagonalization space when acting upon Φ_0,

$$\hat{\mathcal{R}}_n = \sum_\mu r_{\mu,n}\hat{\Omega}_\mu. \tag{23}$$

To obtain the EOM-IP-CC scheme accounting for single and double excitations (EOM-IP-CCSD),[35,37] $\hat{T}$ is chosen to be limited to $\hat{T} = \hat{T}_1 + \hat{T}_2$. Furthermore, the

determinantal basis is limited to all determinants that can be obtained by removing an electron from Φ_0 plus those determinants with one removed and one additionally excited electron, that is,

$$\hat{\mathcal{R}}_n = \sum_i r_{i,n}\hat{a}_i + \frac{1}{2}\sum_{ij}\sum_b r^b_{ji,n}\hat{a}^\dagger_b\hat{a}_j\hat{a}_i\,. \qquad (24)$$

The limitation of the diagonalization space leads to an approximate eigenvalue spectrum. Notably, in comparison to diagonalization of the bare Hamiltonian in the same basis the description of the states is greatly improved.[38–40] A more detailed description of the underlying theory and details on the implementation will be published elsewhere.

III. COMPUTATIONAL DETAILS

The calculations were performed in fully decontracted d-aug-cc-pwCVQZ basis sets (d-aug-cc-pVQZ for H and He).[41–43] The *GW* calculations were performed using spherical shell components, whereas the coupled-cluster calculations were performed using Cartesian Gaussians. To avoid near-linear dependencies, basis functions were removed from the uncontracted sets when the ratio of two exponents within an angular-momentum set was smaller than 1.35. Double augmentation (d-aug) for Li and Be is not available in the literature. For these atoms, we added diffuse functions by means of straightforward extrapolation using the smallest two exponents ζ_{n-1} and ζ_n in each set: $\zeta_{n+1} = \zeta_n^2/\zeta_{n-1}$. Basis sets of the types 8s5p4d3f for H, 9s5p4d3f for He, 14s11p7d5f3g for Li and Be, and 14s10p7d5f3g for B–Ne resulted.

Each *GW* calculation was performed in two independent manners with the program packages QUEST[25,26] and TURBOMOLE,[24] yielding identical results. In the *GW* calculations, the aug-cc-pwCV5Z auxiliary basis set of Hättig[44] was used for the resolution-of-the-identity approximation of the two-electron integrals. The parameter η was set to 0.01 E_h in G_0W_0 calculations and to 0.03 E_h in ev*GW* calculations. The ev*GW* iterations were considered to be converged when changes in the quasiparticle energies of the HOMO and LUMO levels were smaller than 10^{-6} E_h. The PBE0 functional was used to approximate the Kohn–Sham level.[45–47]

With the magnetic field along the z-axis, the Hartree–Fock and Kohn–Sham spin orbitals were constrained to be eigenfunctions of the one-particle angular-momentum and spin operators $\hat{\ell}_z$ and and $\hat{s}_z$. This constraint was also applied to the $B = 0$ case.

The EOM-IP-CCSD calculations were performed with the coupled-cluster code of Hampe and Stopkowicz,[17] which was interfaced to the LONDON program.[27,28]

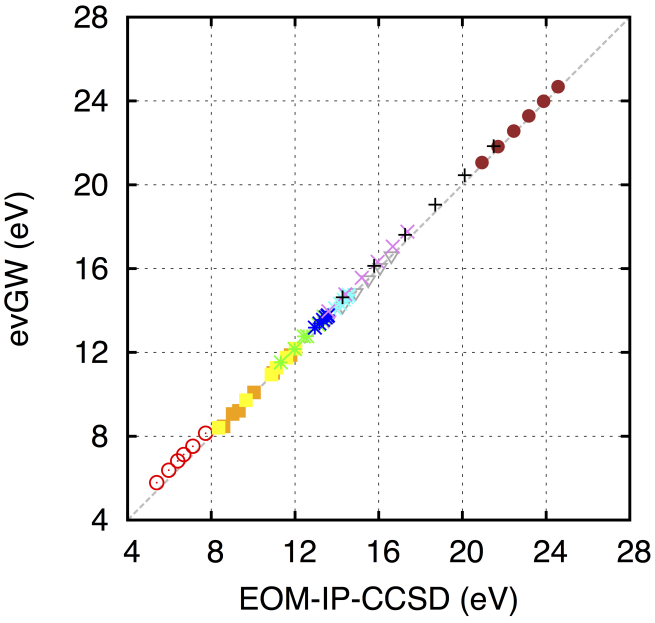

FIG. 1. ev*GW*@PBE0 HOMO quasiparticle energies (eV) plotted against the CCSD reference values. Color code: H = dark gray, He = brown, Li = red, Be = orange, B = yellow, C = green, N = cyan, O = blue, F = violet, Ne = black.

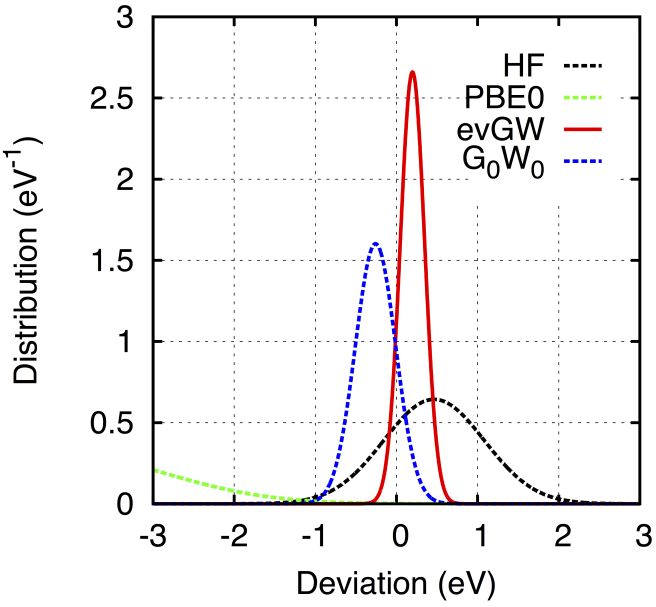

FIG. 2. Normalized Gaussian distributions of the Hartree–Fock, PBE0, ev*GW*, and G_0W_0 deviations from the CCSD reference values.

IV. RESULTS AND DISCUSSION

For all field strengths up to 0.25 B_0 for the CCSD level as well as for the PBE0 and Hartree–Fock (HF) levels, we found the following M_S/M_L quantum numbers for the ground states of the atoms H, He, N, O, F, and Ne: $-\frac{1}{2}/0$,

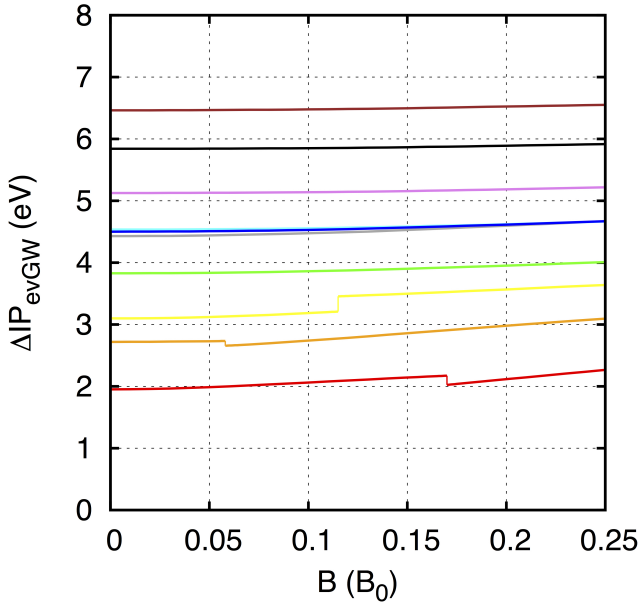

FIG. 3. evGW@PBE0 correction to the Koopmans-like PBE0 ionization potentials (eV) as a function of the magnetic field strength. Color code: H = dark gray, He = brown, Li = red, Be = orange, B = yellow, C = green, N = cyan, O = blue, F = violet, Ne = black.

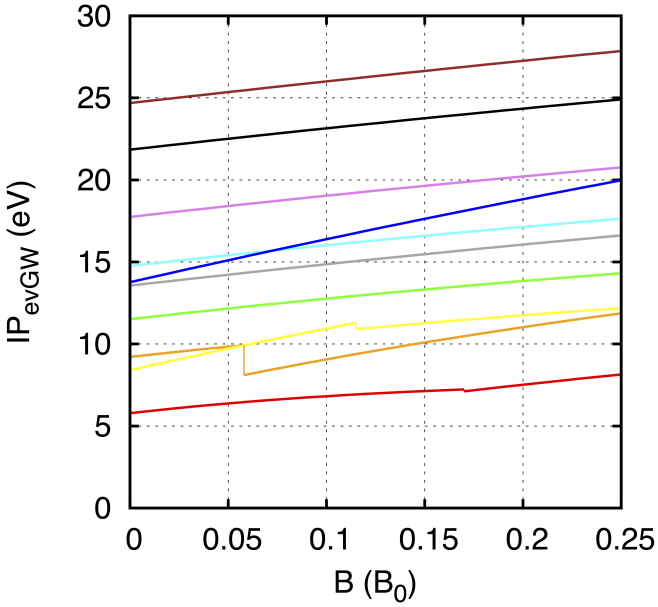

FIG. 4. evGW@PBE0 ionization potentials (eV) as a function of the magnetic field strength. Color code: H = dark gray, He = brown, Li = red, Be = orange, B = yellow, C = green, N = cyan, O = blue, F = violet, Ne = black.

TABLE I. Quantum numbers M_S/M_L for the atoms Li, Be, B, and C as a function of the field strength.

		B/B_0					
		0.00	0.05	0.10	0.15	0.20	0.25
Li	CCSD	$-\frac{1}{2}/0$	$-\frac{1}{2}/0$	$-\frac{1}{2}/0$	$-\frac{1}{2}/0$	$-\frac{1}{2}/-1$	$-\frac{1}{2}/-1$
	PBE0	$-\frac{1}{2}/0$	$-\frac{1}{2}/0$	$-\frac{1}{2}/0$	$-\frac{1}{2}/0$	$-\frac{1}{2}/-1$	$-\frac{1}{2}/-1$
	HF	$-\frac{1}{2}/0$	$-\frac{1}{2}/0$	$-\frac{1}{2}/0$	$-\frac{1}{2}/0$	$-\frac{1}{2}/-1$	$-\frac{1}{2}/-1$
Be	CCSD	0/0	0/0	−1/−1	−1/−1	−1/−1	−1/−1
	PBE0	0/0	0/0	−1/−1	−1/−1	−1/−1	−1/−1
	HF	0/0	−1/−1	−1/−1	−1/−1	−1/−1	−1/−1
B	CCSD	$-\frac{1}{2}/-1$	$-\frac{1}{2}/-1$	$-\frac{1}{2}/-1$	$-\frac{3}{2}/-1$	$-\frac{3}{2}/-1$	$-\frac{3}{2}/-1$
	PBE0	$-\frac{1}{2}/-1$	$-\frac{1}{2}/-1$	$-\frac{1}{2}/-1$	$-\frac{3}{2}/-1$	$-\frac{3}{2}/-1$	$-\frac{3}{2}/-1$
	HF	$-\frac{1}{2}/-1$	$-\frac{1}{2}/-1$	$-\frac{3}{2}/-1$	$-\frac{3}{2}/-1$	$-\frac{3}{2}/-1$	$-\frac{3}{2}/-1$
C	CCSD	−1/−1	−1/−1	−1/−1	−1/−1	−1/−1	−1/−1
	PBE0	−1/−1	−1/−1	−1/−1	−1/−1	−1/−1	−1/−1
	HF	−1/−1	−1/−1	−1/−1	−1/−1	−2/0	−2/0

0/0, $-\frac{3}{2}/0$, −1/−1, $-\frac{1}{2}/-1$, and 0/0, respectively. For the atoms Li, Be, B, and C, changes of the ground state as a function of the magnetic field strength were observed. The respective quantum numbers for each method and field strength are given in Table I.

A. Quasiparticle energies

Tables II and III show the computed quasiparticle energies of the highest occupied molecular orbital (HOMO) at the G_0W_0@PBE0 and evGW@PBE0 levels. The absolute values of these quasiparticle energies refer to IPs with respect to a removed electron at infinite distance, at rest, and without magnetic field. These absolute quasiparticle energies can be compared with the EOM-IP-CCSD results given in Table IV. In Figure 1, the evGW@PBE0 absolute quasiparticle energies are plotted against the EOM-IP-CCSD values, which we regard as reference values. The mean deviation of the evGW@PBE0 values from these reference values amounts to 0.20 eV, and the deviations are scattered with a standard deviation of 0.15 eV about the mean deviation. The mean absolute deviation and the root-mean-square deviation amount to 0.22 and 0.25 eV, respectively.

The evGW@PBE0 HOMO quasiparticle energies are slightly more accurate than their G_0W_0@PBE0 counterparts, which show a mean deviation of −0.25 eV with a standard deviation of 0.25 eV. Figure 2 shows the distributions of the evGW@PBE0 and G_0W_0@PBE0 deviations, assuming that these are Gaussian distributions. In the figure, a comparison is also made with the Hartree–Fock and Kohn–Sham (PBE0) values obtained from Koopmans' theorem (as the negative of the energy of the HOMO). The PBE0 values are very poor (visible in the lower left corner of Figure 2), and the GW quasiparticle energies yield dramatically improved values relative to the EOM-IP-CCSD values. The Hartree–Fock and PBE0

mean deviations are 0.46 and −4.1 eV, respectively, with standard deviations of 0.62 and 1.3 eV.

The error distributions shown in Figure 2 for the atoms H–Ne in various magnetic fields are in accord with the observations made in earlier density-functional theory (DFT), G_0W_0, and evGW studies of ionization potentials of molecules in the absence of external fields, where G_0W_0 is also a dramatic improvement over DFT, and where evGW is also a significant improvement over G_0W_0.[32,33] The correction to the IP by the GW approach is in fact only weakly dependent on the magnetic field strength. This is shown in Figure 3, where the evGW increment (ΔIP) is plotted. Except for Li and Be, the evGW increment is nearly constant in the range $0 \le B \le 0.25\ B_0$. The data used to generate Figure 3 are given in the Supplementary Material.

B. Ionization potentials in a magnetic field

When calculating IPs, we must take into account the energy of the emitted electron in the magnetic field, assuming that the electron goes into the lowest Landau level consistent with the electron's orbital and spin angular momentum. In atomic units, the Landau energy is given by[49]

$$E^{\text{Landau}}_{n,m_\ell,m_s} = \left(n + \tfrac{1}{2}m_\ell + \tfrac{1}{2}|m_\ell| + m_s + \tfrac{1}{2}\right) B\,, \qquad (25)$$

where $n = 0, 1, 2, \ldots$ is the radial quantum number of the electron, $m_\ell = 0, \pm1, \pm2, \ldots$ its orbital angular momentum quantum number, and $m_s = \pm1/2$ its spin angular momentum quantum number. Assuming no motion in the field direction, the lowest energy of the emitted electron is given by $\left(\frac{1}{2}m_\ell + \frac{1}{2}|m_\ell| + m_\text{s} + \frac{1}{2}\right) B$. Noting that the electron's Zeeman energy is given by $\left(\frac{1}{2}m_\ell + m_\text{s}\right) B$, we may view the remainder $\left(\frac{1}{2}|m_\ell| + \frac{1}{2}\right) B \ge 0$ as the diamagnetic contribution to the Landau energy, the zero-point energy $\frac{1}{2}B$ arising from the confinement of the electron by the magnetic field. For negative orbital angular momentum $m_\ell < 0$, the negative orbital Zeeman energy is cancelled by a diamagnetic contribution, giving rise to an infinite degeneracy of Landau levels with non-positive m_ℓ.

Within the GW approximation, the IP of an atom in a magnetic field B is now given by

$$\begin{aligned}\text{IP}_{m_\ell,m_s}(B) = &-\varepsilon_{m_\ell,m_s}(B) \\ &+ \tfrac{1}{2}\left(m_\ell + |m_\ell| + 2m_s + 1\right) B\,, \end{aligned} \qquad (26)$$

where $\varepsilon_{m_\ell,m_s}(B)$ is the GW quasiparticle energy of the ionized orbital and $\frac{1}{2}\left(m_\ell + |m_\ell| + 2m_s + 1\right) B$ the Landau energy of the emitted electron. The ionization threshold for a given electronic state is the lowest IP of the atom, bearing in mind that the ionization with the lowest IP may not be from the HOMO but from a lower spin orbital of different angular momentum if this gives a lower Landau energy.[12,13]

In Figure 4, we have plotted the lowest IP of each atom H to Ne calculated at the evGW@PBE0 level of theory for field strengths $B \le 0.25\ B_0$. The data used to generate Figure 4 are given in the Supplementary Material. The IPs increase monotonically with increasing field strength except for discontinuous changes when the ground state changes, which in the plotted interval occurs for Li, B, and Be. At $B = 0.170\ B_0$, the IP of Li changes from 7.23 to 7.11 eV, at $B = 0.058\ B_0$, the IP of Be changes from 9.92 to 8.10 eV, and at $B = 0.115\ B_0$, the IP of B changes from 11.29 to 10.91 eV. Information about the electronic states of the atoms and the ionization processes is given in Table V.

From the plots in Figure 4, we see that the IPs increase in a near-linear manner with increasing field strength. To understand this behavior, we note that the electron's Zeeman energy $\frac{1}{2}m_\ell B + m_s B$ is conserved in the ionization process. Subtracting this energy contribution from the quasiparticle energy $\varepsilon_{m_\ell,m_s}(B)$ to obtain $\varepsilon^{\text{dia}}_{m_\ell,m_s}(B)$ and from the Landau energy in Eq. (26), we arrive at the following expression for the IP:

$$\text{IP}_{m_\ell,m_s}(B) = -\varepsilon^{\text{dia}}_{m_\ell,m_s}(B) + \tfrac{1}{2}\left(|m_\ell| + 1\right) B\,. \qquad (27)$$

Since $\varepsilon^{\text{dia}}_{m_\ell,m_s}(B)$ depends quadratically on B for small B, it has a zero slope at $B = 0$. The initial slope of the IP curves in Figure 4 is therefore equal to $\frac{1}{2}|m_\ell| + \frac{1}{2}$. With increasing field strength, this slope decreases slightly, in a concave manner. In the considered field interval, therefore, the field dependence of the IPs is dominated by the linearity of the Landau energy $\frac{1}{2}\left(|m_\ell| + 1\right) B$, with a much smaller quadratic contribution from the quasiparticle energy. We conclude that, for the field strengths considered here, the increased stability of atoms to ionization in a magnetic field is caused by an increase in the zero-point Landau energy of the emitted electron rather than by changes in the atom.

For the atoms considered by us, the slope of the IP curve is approximately one half atomic unit for ionization from 1s, 2s, or 2p_0 but one atomic unit for ionization from 2p_{-1}, as occurs for the Li atom in the ^2P state, the Be atom in the ^3P state, the B atom in the ^2P state, and for the O atom in the ^3P state; see Figure 4 and Table V.

As anticipated, ionization in a magnetic field does not always occur from the HOMO. Specifically, in a sufficiently strong magnetic field $B \le 0.25\ B_0$, we found that C, N, and Ne do not ionize from the $2\text{p}_{\pm1}$ HOMO but from the lower-lying 2p_0 orbital, whose ionized electron has a smaller Landau energy.

Since the Zeeman energy is conserved upon ionization, the ionization of He occurs with equal probability from the $1\text{s}\alpha$ and $1\text{s}\beta$ spin orbitals. Likewise, Be ionizes from $2\text{s}\alpha$ and $2\text{s}\beta$, while Ne ionizes from $2\text{p}_0\alpha$ and $2\text{p}_0\beta$.

Interestingly, there are only two distinct IP values from the six 2p spin orbitals of Ne: the lowest, doubly degenerate IP from $2\text{p}_0\alpha$ and $2p_0\beta$ and the higher, quadruply degenerate IP from $2p_{\pm1}\alpha$ and $2p_{\pm1}\beta$.

C. Comparison with literature values

There are many studies of ionization energies of neutral atoms and their ions in strong magnetic fields – in particular, for H, He, Li, and Be. We compare mostly with the FCI results of Schmelcher and coworkers for helium,[9,11] for lithium[12] and for beryllium.[13] The extensive studies of Ivanov and Schmelcher for H–He at the Hartree–Fock level of theory and of Schimerczek *et al.*[14] for He–Fe at the DMC level of theory assume near cylindrical symmetry of the atoms rather than near spherical symmetry as assumed by us. Their studies are therefore for fields stronger than those considered by us (at least $B \geq 0.5\ B_0$ rather than $B \leq 0.25\ B_0$) and not relevant for comparisons with our study.

Our evGW/PBE0 and EOM-IP-CCSD ionization energies for helium agree well with the FCI values of Becken *et al.*[9] and the explicitly correlated values of Zhao *et al.*,[50] the EOM-IP-CCSD results being 0.012–0.014 eV lower than the FCI results and about 0.022 eV lower than the explicitly correlated results over the range $0 \leq B \leq 0.25\ B_0$. The evGW/PBE0 ionization energies are about 0.1 eV larger than the FCI and explicitly correlated values in this range.

For the lithium atom, the crossover from ^{2}S to ^{2}P occurs at 0.17 B_0 in our PBE0 calculations and at 0.19 B_0 in the FCI calculations of Al-Hujaj and Schmelcher.[12] In the ^{2}S state at field strengths 0, 0.05 B_0, 0.10 B_0, and 0.15 B_0, the EOM-IP-CCSD ionization energies of 5.39, 5.97, 6.39 and 6.68 eV agree roughly with the FCI values of 5.46, 6.13, 6.54, and 6.89 eV (the last value interpolated). The corresponding evGW@PBE0 values are 5.78, 6.38, 6.82, and 7.13 eV. The variable differences between the evGW/PBE0 and FCI calculations reflect a less smooth field dependence of the ionization potential in the FCI calculations than in the evGW@PBE0 calculations plotted in Figure 4. See also Figure S1 in the Supplementary Material. For the ^{2}P state, the EOM-IP-CCSD ionization potential of 7.12 eV obtained at 0.2 B_0 compares well with FCI result of 7.11 eV; no other comparisons are possible for this state. Recently, Salas *et al.*[20] presented explicitly correlated calculations on lithium in the ^{2}S state, but a graphical representation makes a comparison with our results difficult.

For the beryllium atom, there are, in addition to the FCI calculations by Al-Hujaj and Schmelcher,[13] full-core-plus-correlation (FCPC) calculations by Wang and Qiao.[51] Our evGW@PBE0 and EOM-IP-CCSD singlet ionization potentials agree rather poorly with the FCI results, the EOM-IP-CCSD values of 9.32 eV at zero field and 9.95 eV at 0.05 B_0 being considerably higher than the corresponding FCI values of 8.59 and 9.28 eV. The agreement is better with the FCPC values of 9.19 and 9.81 eV (interpolated) at zero field and at 0.05 B_0, respectively.[51] In view of the constant shift of 0.13–0.14 eV of the EOM-IP-CCSD values relative to the FCPC values, and since our EOM-IP-CCSD value of 9.323 eV at zero field agrees to within 0.001 eV with the experimental IP of Be (see Ref. 48), we consider the EOM-IP-CCSD values more accurate than the FCI and FCPC values. For ionization from the triplet state, the agreement between the EOM-IP-CCSD and FCI results is better than for ionization from the singlet state. At 0.1 B_0 and 0.2 B_0, our EOM-IP-CCSD ionization energies of 9.02 and 10.96 eV are slightly higher than the FCI values 8.82 and 10.72 eV, respectively. Wang and Qiao report the values 8.83 and 10.76 eV for these field strengths.[51]

V. CONCLUSIONS

We have computed quasiparticle energies of the atoms H–Ne in the presence of a magnetic field of strength $B \leq 0.25\ B_0$ at the GW levels of theory, comparing with HF, DFT, and EOM-IP-CCSD calculations. The corresponding first ionization energies have been calculated, analysed, and compared with available literature data. Our study is the first systematic study of ground-state ionization potentials for first row atoms at field strengths appropriate for magnetic white dwarfs.

Our study shows that the evGW@PBE0 model provides quasiparticle energies in good agreement with CCSD values, slightly outperforming the G_0W_0@PBE0 model. These values are more accurate than those obtained from HF theory and represent a substantial improvement over density-functional values using the PBE0 functional, which significantly underestimate ionization potentials. Our EOM-IP-CCSD ionization energies agree well with the best literature data, giving a uniformly good description of the ionization potentials of the first-row atoms in a magnetic fields of strength $B \leq 0.25\ B_0$. At these field strengths, the ionization potentials increase in a near-linear fashion with the applied field, arising from the linear dependence of the Landau energy of the ionized electron in the field. The increased stability of atoms under such conditions therefore arises mostly from the increased energy of the ionized electron rather than from changes in the electronic structure of the atom.

SUPPLEMENTARY MATERIAL

See supplementary material for all of the raw data that have been used to generate Figures 3 and 4. Figure S1 compares the present work's results for Li with data from the literature.

ACKNOWLEDGMENTS

C.H. gratefully acknowledges financial support by the Deutsche Forschungsgemeinschaft (DFG) through the

Priority Programme 1807 "Control of London Dispersion Interactions in Molecular Chemistry" (Grant No. KL 721/5-2). A.M.T. is grateful for support from a Royal Society Research Fellowship and the European Research Council under H2020/ERC Consolidator Grant "topDFT" (Grant No. 772259). S.S. gratefully acknowledges financial support by the DFG through Grant No. STO 1239/1-1. This work was supported by the Norwegian Research Council through the CoE Hylleraas Centre for Quantum Molecular Sciences Grant No. 262695.

[1] L. Ferrario, D. de Martino, and B. T. Gänsicke, Space Sci. Rev. **191**, 111 (2015).
[2] P. Schmelcher, Int. J. Quantum Chem. **70**, 789 (1998).
[3] D. Lai, Rev. Mod. Phys. **73**, 022505 (2000).
[4] A. Thirumalai and J. S. Heyl, Adv. At. Mol. Opt. Phy. **63**, 323 (2014).
[5] M. V. Ivanov and P. Schmelcher, Phys. Rev. A **57**, 3793 (1998).
[6] M. V. Ivanov and P. Schmelcher, Phys. Rev. A **61**, 022505 (2000).
[7] M. V. Ivanov and P. Schmelcher, J. Phys. B: At. Mol. Opt. Phys. **34**, 2031 (2001).
[8] M. V. Ivanov and P. Schmelcher, Eur. Phys. J. D **14**, 279 (2001).
[9] W. Becken, P. Schmelcher, and F. K. Diakonos, J. Phys. B: At. Mol. Opt. Phys. **32**, 1557 (1999).
[10] W. Becken and P. Schmelcher, J. Phys. B: At. Mol. Opt. Phys. **33**, 545 (2000).
[11] W. Becken and P. Schmelcher, Phys. Rev. A **63**, 053412 (200).
[12] O.-A. Al-Hujaj and P. Schmelcher, Phys. Rev. A **70**, 033411 (2004).
[13] O.-A. Al-Hujaj and P. Schmelcher, Phys. Rev. A **70**, 023411 (2004).
[14] C. Schimeczek, S. Boblest, D. Meyer, and G. Wunner, Phys. Rev. A **88**, 012509 (2013).
[15] S. Boblest, C. Schimeczek, and G. Wunner, Phys. Rev. A **89**, 012505 (2014).
[16] S. Stopkowicz, J. Gauss, K. K. Lange, E. I. Tellgren, and T. Helgaker, J. Chem. Phys. **143**, 074110 (2015).
[17] F. Hampe and S. Stopkowicz, J. Chem. Phys. **146**, 154105 (2017).
[18] A. Scrinzi, Phys. Rev. A **58**, 3879 (1998).
[19] Y. Tang, L. Wang, X. Song, X. Wang, Z.-C. Yan, and H. Qiao, Phys. Rev. A **87**, 042518 (2013).
[20] J. A. Salas, I. Pelaschier, and K. Varga, Phys. Rev. A **92**, 033401 (2015).
[21] S. Doma, M. O. Shaker, A. M. Farag, and F. N. El-Gammal, Acta Phys. Pol. A **126**, 700 (2014).
[22] S. Doma, M. O. Shaker, A. M. Farag, and F. N. El-Gammal, J. Exp. Theor. Phys. **124**, 1 (2017).
[23] A. Thirumalai and J. S. Heyl, Mon. Not. R. Astron. Soc. **407**, 590 (2010).
[24] TURBOMOLE Version 7.3 (July 2018), a development of University of Karlsruhe (TH) and Forschungszentrum Karlsruhe GmbH, 1989-2007, TURBOMOLE GmbH, since 2007, available from http://www.turbomole.com.
[25] T. J. P. Irons, J. Zemen, and A. M. Teale, J. Chem. Theory and Comput. **13**, 3636 (2017).
[26] QUEST, A rapid development platform for Quantum Electronic Structure Techniques, 2017 (see https://quest.codes/ for more information).
[27] E. I. Tellgren (primary author), T. Helgaker, A. Soncini, K. K. Lange, A. M. Teale, U. E. Ekström, Stopkowicz, J. H. Austad, and S. Sen, A quantum-chemistry program for plane-wave/GTO hybrid basis sets and finite magnetic field calculations (see londonprogram.org for more information).
[28] E. I. Tellgren, A. Soncini, and T. Helgaker, J. Chem. Phys. **129**, 154114 (2008).
[29] M. Vincke and D. Baye, J. Phys. B: At. Mol. Opt. Phys. **21**, 2407 (1988).
[30] D. Baye and M. Vincke, J. Phys. B: At. Mol. Opt. Phys. **23**, 2467 (1990).
[31] L. Hedin, Nucl. Instr. Meth. Phys. Res. A **308**, 169 (1991).
[32] X. Blase, C. Attaccalite, and V. Olevano, Phys. Rev. B **83**, 115103 (2011).
[33] M. J. van Setten, F. Weigend, and F. Evers, J. Chem. Theory Comput. **9**, 232 (2012).
[34] K. Krause, M. E. Harding, and W. Klopper, Mol. Phys. **113**, 1952 (2015).
[35] J. F. Stanton and J. Gauss, J. Chem. Phys. **101**, 8938 (1994).
[36] T. D. Crawford and H. F. Schaefer III, Rev. Comp. Chem. **14**, 33 (2000).
[37] R. P. Mattie, Ph.D. thesis, University of Florida (1995).
[38] H. Koch, H. J. Aa. Jensen, P. Jørgensen, and T. Helgaker, J. Chem. Phys. **93**, 3345 (1990).
[39] J. F. Stanton and R. J. Bartlett, J. Chem. Phys. **98**, 7029 (1993).
[40] D. C. Comeau and R. J. Bartlett, Chem. Phys. Lett. **207**, 414 (1993).
[41] B. P. Prascher, D. E. Woon, K. A. Peterson, T. H. Dunning Jr., and A. K. Wilson, Theor. Chem. Acc. **128**, 69 (2011).
[42] K. A. Peterson and T. H. Dunning Jr., J. Chem. Phys. **117**, 10548 (2002).
[43] D. E. Woon and T. H. Dunning Jr., J. Chem. Phys. **100**, 2975 (1994).
[44] C. Hättig, Phys. Chem. Chem. Phys. **7**, 59 (2005).
[45] J. P. Perdew, M. Ernzerhof, and K. Burke, J. Chem. Phys. **105**, 9982 (1996).
[46] M. Ernzerhof and G. E. Scuseria, J. Chem. Phys. **110**, 5029 (1999).
[47] C. Adamo and V. Barone, J. Chem. Phys. **110**, 6158 (1999).
[48] W. Klopper, R. A. Bachorz, D. P. Tew, and C. Hättig, Phys. Rev. A **81**, 022503 (2010).
[49] R. H. Garstang, Rep. Prog. Phys. **40**, 105 (1977).
[50] J.-J. Zhao, X.-F. Wang, and H.-X. Qiao, Chin. Phys. B **19**, 113102 (2010).
[51] X.-F. Wang and H.-X. Qiao, Few-Body Syst. **53**, 453 (2012).

TABLE II. G_0W_0@PBE0 quasiparticle energies (in eV) of the HOMO level as a function of the magnetic-field strength.

		B/B_0					
Atom	IP[a]/eV	0.00	0.05	0.10	0.15	0.20	0.25
H	13.606	−13.16	−13.83	−14.48	−15.11	−15.71	−16.29
He	24.592	−24.05	−23.36	−22.66	−21.95	−21.21	−20.47
Li	5.392	−5.73	−6.34	−6.81	−7.14	−7.49	−8.13
Be	9.323	−9.13	−8.40	−8.77	−9.81	−10.75	−11.61
B	8.300	−8.01	−9.34	−10.57	−10.89	−11.39	−11.84
C	11.267	−11.01	−11.67	−12.28	−12.85	−13.38	−12.57
N	14.553	−14.14	−14.12	−14.05	−13.93	−13.76	−13.55
O	13.618	−13.19	−13.17	−13.11	−13.00	−12.85	−12.65
F	17.441	−17.08	−16.37	−15.65	−14.91	−14.13	−13.33
Ne	21.616	−21.06	−19.68	−18.28	−16.85	−15.38	−13.89

a) Zero-field CCSDTQ5 ionization potential from Ref. 48.

TABLE III. evGW@PBE0 quasiparticle energies (in eV) of the HOMO level as a function of the magnetic-field strength.

		B/B_0					
Atom	IP[a]/eV	0.00	0.05	0.10	0.15	0.20	0.25
H	13.606	−13.56	−14.22	−14.86	−15.47	−16.06	−16.62
He	24.592	−24.68	−23.99	−23.29	−22.56	−21.82	−21.06
Li	5.392	−5.78	−6.38	−6.82	−7.13	−7.52	−8.14
Be	9.323	−9.21	−8.47	−9.06	−10.09	−11.03	−11.87
B	8.300	−8.40	−9.72	−10.94	−11.27	−11.75	−12.18
C	11.267	−11.51	−12.16	−12.77	−13.32	−13.71	−12.76
N	14.553	−14.75	−14.72	−14.64	−14.51	−14.33	−14.11
O	13.618	−13.77	−13.74	−13.67	−13.55	−13.38	−13.18
F	17.441	−17.74	−17.05	−16.32	−15.56	−14.77	−13.96
Ne	21.616	−21.84	−20.47	−19.05	−17.61	−16.14	−14.63

a) Zero-field CCSDTQ5 ionization potential from Ref. 48.

TABLE IV. EOM-IP-CCSD reference values (in eV) as a function of the magnetic-field strength.

		B/B_0					
Atom	IP[a]/eV	0.00	0.05	0.10	0.15	0.20	0.25
H	13.606	13.60	14.27	14.90	15.50	16.06	16.60
He	24.592	24.57	23.88	23.17	22.45	21.70	20.94
Li	5.392	5.39	5.97	6.39	6.68	7.12	7.73
Be	9.323	9.32	8.59	9.02	10.04	10.96	11.79
B	8.300	8.35	9.66	10.87	11.11	11.59	12.02
C	11.267	11.32	11.98	12.58	13.13	13.37	12.42
N	14.553	14.57	14.55	14.46	14.33	14.14	13.91
O	13.618	13.57	13.55	13.47	13.34	13.17	12.95
F	17.441	17.37	16.67	15.95	15.19	14.40	13.59
Ne	21.616	21.49	20.11	18.70	17.26	15.78	14.27

a) Zero-field CCSDTQ5 ionization potential from Ref. 48.

TABLE V. IPs of the first-row atoms in their ground states up to field strength $B = 0.25\ B_0$. For each atom, we have listed the zero-field term symbol and ground-state electron configuration, the ionized spin orbital (ISO), its order number n in HOMO-n, the Landau energy, and the initial IP slope in units of E_h/B_0. When more than one ground state exists in the considered field range, we give information on each state.

Atom	Field	Electronic State[a]	ISO[b]	HOMO-n	Landau	Slope
H		^{2}S($1s^1$)	$1s\beta$	0	0	$\frac{1}{2}$
He		^{1}S($1s^2$)	$1s\alpha$	0	B	$\frac{1}{2}$
			$1s\beta$	1	0	$\frac{1}{2}$
Li	≤ 0.170	^{2}S($1s^2 2s^1$)	$2s\beta$	0	0	$\frac{1}{2}$
	≥ 0.170	^{2}P($1s^2 2p_{-1}^1$)	$2p_{-1}\beta$	0	0	1
Be	≤ 0.058	^{1}S($1s^2 2s^2$)	$2s\alpha$	0	B	$\frac{1}{2}$
			$2s\beta$	1	0	$\frac{1}{2}$
	≥ 0.058	^{3}P($1s^2 2s^1 2p_{-1}^1$)	$2p_{-1}\beta$	0	0	1
B	≤ 0.115	^{2}P($1s^2 2s^2 2p_{-1}^1$)	$2p_{-1}\beta$	0	0	1
	≥ 0.115	^{4}P($1s^2 2s^1 2p_{-1}^1 2p_0^1$)	$2p_0\beta$	0	0	$\frac{1}{2}$
C		^{3}P($1s^2 2s^2 2p_{-1}^1 2p_0^1$)	$2p_0\beta$	0, 1	0	$\frac{1}{2}$
N		^{4}S($1s^2 2s^2 2p_{-1}^1 2p_0^1 2p_{+1}^1$)	$2p_0\beta$	1, 2	0	$\frac{1}{2}$
O		^{3}P($1s^2 2s^2 2p_{-1}^2 2p_0^1 2p_{+1}^1$)	$2p_{-1}\alpha$	0	B	1
F		^{2}P($1s^2 2s^2 2p_{-1}^2 2p_0^2 2p_{+1}^1$)	$2p_0\alpha$	0	B	$\frac{1}{2}$
Ne		^{1}S($1s^2 2s^2 2p_{-1}^2 2p_0^2 2p_{+1}^2$)	$2p_0\alpha$	1	B	$\frac{1}{2}$
			$2p_0\beta$	4	0	$\frac{1}{2}$

[a] Single occupied spin orbitals have beta spin. Zero-field notation used.

[b] All degenerate ionization processes are given.